

Parameterizations of Sea-Spray Impact on the Air–Sea Momentum and Heat Fluxes

J.-W. BAO, C. W. FAIRALL, S. A. MICHELSON, AND L. BIANCO

NOAA/ESRL, Boulder, Colorado

(Manuscript received 4 January 2011, in final form 16 June 2011)

ABSTRACT

This paper focuses on parameterizing the effect of sea spray at hurricane-strength winds on the momentum and heat fluxes in weather prediction models using the Monin–Obukhov similarity theory (a common framework for the parameterizations of air–sea fluxes). In this scheme, the mass-density effect of sea spray is considered as an additional modification to the stratification of the near-surface profiles of wind, temperature, and moisture in the marine surface boundary layer (MSBL). The overall impact of sea-spray droplets on the mean profiles of wind, temperature, and moisture depends on the wind speed at the level of sea-spray generation. As the wind speed increases, the mean droplet size and the mass flux of sea-spray increase, rendering an increase of stability in the MSBL and the leveling-off of the surface drag. Sea spray also tends to increase the total air–sea sensible and latent heat fluxes at high winds. Results from sensitivity testing of the scheme in a numerical weather prediction model for an idealized case of hurricane intensification are presented along with a dynamical interpretation of the impact of the parameterized sea-spray physics on the structure of the hurricane boundary layer.

1. Introduction

The energy transfer through the air–sea interface, cast in terms of heat and momentum fluxes in weather prediction models, is a major controlling factor of hurricane intensification. Results from theoretical studies (see Emanuel 1995) suggest that the ratio of enthalpy bulk transfer coefficient to surface drag coefficient must be in the range of 0.75–1.25 in order for simulated hurricanes to be of realistic intensity. However, the observed value of this ratio over the sea is between 0.6 and 0.7 at moderate wind speeds within the range in which reliable direct flux measurements exist (Black et al. 2007). While observational determination of the ratio is not available for 10-m winds beyond 30 m s^{-1} because of technical difficulties, the use of the traditional bulk formulations for the enthalpy transfer and drag coefficients results in the ratio decreasing significantly below 0.7 at extreme wind speeds ($>40 \text{ m s}^{-1}$). One possibility for this discrepancy is the failure of the traditional bulk transfer coefficients to take into account the effect of sea spray (Fairall et al. 2009).

The omnipresence of sea spray in the marine surface boundary layer (MSBL) has long been observed under

hurricane-strength winds. In contrast, the effect of sea spray on the air–sea momentum and heat fluxes at hurricane-strength winds and how the effect is parameterized in numerical weather prediction (NWP) models are relatively new subjects of very active investigation. High surface winds ($>30 \text{ m s}^{-1}$) generate large reentrant sea-spray droplets (Fairall et al. 2009), which tend to increase the sea–air enthalpy transfer and, thus, have a positive feedback to the intensification of hurricanes (Andreas and Emanuel 2001). On the other hand, sea spray is generated at the expense of the momentum of turbulence at the air–sea interface, which inevitably causes the air–sea turbulent momentum flux to change. The combined feedback effect of sea spray on the overall air–sea momentum and enthalpy fluxes has not been well understood since such a combination, in general, adds to the complexity of air–sea interaction. It is interesting to note that because of the difficulty in making observations in the hurricane surface layer, the evaluation of the importance of sea-spray effect has been performed using NWP model simulations of tropical cyclones and the results from these simulations are, to a great degree, dependent on their representation in numerical models (e.g., Bao et al. 2000; Wang et al. 2001).

Powell et al. (2003) presents an analysis of the air–sea momentum transfer as a function of 10-m wind speed for high winds in tropical cyclones using the wind profiles

Corresponding author address: Jian-Wen Bao, NOAA/ESRL, 325 Broadway, Boulder, CO 80305.
E-mail: jian-wen.bao@noaa.gov

measured by global positioning system (GPS) sondes. They find that the surface drag coefficient levels off as the wind speeds increase above 35 m s^{-1} . This finding is contrary to surface flux parameterizations that are currently used in NWP models. They speculate that sea spray may play an important role in this behavior. Analysis of the measurements from the Slope to Shelf Energetics and Exchange Dynamics (SEED) project (Jarosz et al. 2007) confirms the trend of the dependence of the drag coefficient on 10-m winds that is revealed by Powell et al. (2003). Makin (2005) and Andreas (2004) further confirm that the consideration of the sea-spray effect on the air–sea momentum transfer does lead to the trend of the dependence of the drag coefficient on 10-m winds that is similar to that presented in Powell et al. (2003). Despite the technical challenges in making direct observations of the modification of sea spray to air–sea heat and moisture fluxes at high winds, recent measurements of bulk air–sea fluxes of momentum and heat from the Coupled Boundary Layers Air–Sea Transfer (CBLAST; Black et al. 2007) strongly suggest a different trend of the dependence of the heat exchange coefficient on 10-m winds that is widely used in NWP models (Zhang et al. 2008). All these studies point out the need to account for the effect of sea spray in the calculations of air–sea momentum and enthalpy fluxes in NWP models.

In this paper, we propose that the effect of sea spray be considered as an additional modification to the stratification of the profiles of wind, temperature, and moisture in the MSBL, and thus they can be parameterized in NWP models using a common framework of parameterizations of air–sea fluxes: the Monin–Obukhov similarity theory. The proposed parameterization scheme assumes that wave breaking and sea-spray generation takes place on the subgrid scale, and the air drag that accelerates sea spray is part of the air–sea interfacial stress. Sea-spray generation due to wave breaking is associated with turbulent gusty flows that are related, but not equal, to the grid-resolved mean flows through the so-called subgrid Reynolds stress in the governing equations for the grid-resolved flows.

This paper is intended to 1) describe how the effect of sea spray is parameterized in a hurricane NWP model, and 2) demonstrate numerically how sensitive the model simulated surface fluxes and atmospheric boundary layer (ABL) structure are to the parameterized effect in an idealized simulation of hurricane intensification. The rest of the paper is organized as follows: in the next section, the overall effect of sea spray on dynamics in the MSBL is discussed in the context of the budget equation of turbulence kinetic energy (TKE) and its connection with the Monin–Obukhov similarity theory; the parameterization

of the sea-spray effect on sensible and moisture heat fluxes is described in section 3; section 4 presents the parameterization of the sea-spray effect on the momentum flux; section 5 summarizes the physical attributes of the parameterization scheme that includes the parameterized effect as introduced in the previous two sections; section 6 presents the results from three sensitivity simulations using a commonly used NWP model to numerically demonstrate and dynamically interpret the impact of sea spray on the intensification of tropical cyclones; and conclusions are provided in section 7.

2. Dynamical and thermal effect of sea spray

The dynamical aspects of sea spray can be addressed through the budget equation of TKE in the MSBL, which in the absence of sea spray, is governed approximately by

$$-\langle uw \rangle \frac{\partial U}{\partial z} + \frac{g \langle \theta_v w \rangle}{\Theta_v} - \frac{\partial}{\partial z} \left(\frac{\langle Ew \rangle}{2} + \frac{\langle pw \rangle}{\rho} \right) - \varepsilon = \frac{DE}{Dt}, \quad (2.1)$$

where z is the vertical coordinate; $\langle \rangle$ denotes mean (following the Reynolds convention); E is twice the TKE; U is the mean horizontal velocity of air motion; u and w are the eddy components of U and the vertical air motion, respectively; Θ_v and θ_v are the mean and eddy components of virtual potential temperature, respectively; p and ρ are the pressure and density of air (including moisture), respectively; ε is the dissipation rate of TKE; and g is the acceleration of gravity. The virtual potential temperature used here is defined as dry potential temperature multiplied by $(1 + 0.608q - q_l)$, where q is the mass fraction of water vapor in the air (i.e., the specific humidity) and q_l is the mass fraction of liquid water. The right-hand side of Eq. (2.1) is the total derivative of E . Here details of the complex wavy geometry of the sea surface are ignored by treating the quantities of interest in an average sense (Mueller and Veron 2009).

When sea spray is present in the MSBL, the budget equation of TKE is rendered into the following form:

$$-\langle uw \rangle \frac{\partial U}{\partial z} + \left(\frac{g \langle \theta_v w \rangle}{\Theta_v} + \frac{g \langle \theta_{v,sp} w \rangle}{\Theta_v} \right) - \frac{\partial}{\partial z} \left(\frac{\langle Ew \rangle}{2} + \frac{\langle pw \rangle}{\rho} \right) - (\varepsilon + g\sigma V_f S) = \frac{DE}{Dt}, \quad (2.2)$$

where $\theta_{v,sp}$ is the perturbation in virtual potential temperature caused by heat transfer between air (of virtual potential temperature Θ_v) and sea spray (of mean virtual potential temperature $\theta_{v,sp}$ at the droplet surface),

$\sigma = (\rho_w - \rho)/\rho$ is the relative excess of the density of seawater ρ_w over the density of air, V_f is the fall speed of sea-spray droplets, and S is the volumetric concentration of sea-spray mass. The last term including V_f represents the rate at which turbulent energy is consumed for spray droplets to be suspended in the flow against gravity (see, e.g., Adams and Weatherly 1981). This equation shows that the impact of sea spray on the budget equation of TKE is taken into account by adding an additional term to the buoyancy production and an additional term in the dissipation due to the suspension of sea spray by turbulence.

After a simple rearrangement of the above equation using the friction velocity u_* defined as $\sqrt{-\langle uw \rangle}$, one can obtain the following dimensionless budget equation of TKE:

$$\frac{\kappa z}{u_*} \frac{\partial U}{\partial z} + \frac{\kappa z}{u_*^3} \left(\frac{g \langle \theta_v w \rangle}{\Theta_v} + \frac{g \langle \theta_{v,sp} w \rangle}{\Theta_v} - g \sigma V_f S \right) - \frac{\kappa z}{u_*^3} \frac{\partial}{\partial z} \left(\frac{\langle Ew \rangle}{2} + \frac{\langle pw \rangle}{\rho} \right) - \frac{\kappa z}{u_*^3} \varepsilon = \frac{\kappa z}{u_*^3} \frac{DE}{Dt}, \quad (2.3)$$

where κ is the von Kármán constant. The second term of the left-hand side can be expressed as $-z/L$, where L is defined as

$$L = - \frac{u_*^3}{\kappa \left(\frac{g \langle \theta_v w \rangle}{\Theta_v} + \frac{g \langle \theta_{v,sp} w \rangle}{\Theta_v} - g \sigma V_f S \right)} \quad (2.4)$$

and has a dimension of length.

An important aspect of the dimensionless TKE budget equation is that each of the dimensionless terms in the equation should depend only on a dimensionless parameter z/L . In fact, in the absence of sea spray (i.e., $g \langle \theta_{v,sp} w \rangle / \Theta_v = 0$ and $g \sigma V_f S = 0$), this equation connects the scaling argument of the Monin–Obukhov similarity theory and the dynamical aspect of the budget equation of TKE in the surface boundary layer. This equation suggests that the parameterizations of the feedback effect of sea spray on the momentum and heat fluxes can be based on the following assumption: the turbulent eddies responsible for turbulence mixing are mostly generated by shear and the variations of static stability due to sea-spray loading modify the log profiles of wind, temperature, and moisture corresponding to the so-called neutral stratification. As noted by Stull (1997), the Monin–Obukhov similarity theory is based on the same assumption that takes into account the feedback effect (i.e., modifications) of variations in static stability caused by turbulent heat fluxes to the log profiles of wind

and temperature. Given the prominent role that the Monin–Obukhov similarity theory plays in the calculation of the momentum and heat fluxes in the MSBL, it is natural to consider the feedback effect of sea spray on the fluxes by assuming that the Monin–Obukhov similarity theory is still valid in the sea-spray-laden MSBL, provided the length scale parameter is chosen properly. Therefore, if we define $L_{MO} = -u_*^3 / \kappa (g \langle \theta_{v,sp} w \rangle / \Theta_v)$, and Θ_v and θ_v are the mean and eddy components of virtual potential temperature, respectively; Θ and θ are the mean and eddy components of potential temperature, respectively; and Q and q are the mean and eddy components of specific humidity, respectively; the conventional Monin–Obukhov similarity relations [with $\phi_m(z/L_{MO})$, and $\phi_h(z/L_{MO})$ and $\phi_c(z/L_{MO})$ being functions of z/L_{MO}],

$$\begin{aligned} \frac{\kappa z}{u_*} \frac{\partial U}{\partial z} &= \phi_m(z/L_{MO}), \\ \frac{\kappa z u_*}{-\langle \theta w \rangle_*} \frac{\partial \Theta}{\partial z} &= \phi_h(z/L_{MO}), \quad \text{and} \\ \frac{\kappa z u_*}{-\langle qw \rangle_*} \frac{\partial Q}{\partial z} &= \phi_c(z/L_{MO}), \end{aligned} \quad (2.5)$$

can be extended to include the sea-spray effect by replacing the conventional Monin–Obukhov length L_{MO} with L as defined previously [Eq. (2.4)]. The parameterizations of the feedback effect of sea spray on the momentum and heat fluxes come down to the parameterizations of the sea-spray modification to the fluxes and mean profiles calculated using the conventional Monin–Obukhov similarity relations. That is, in the presence of sea spray and ignoring the wavy geometric effect of water surface, both the formulations of the MSBL momentum, sensible heat, and moisture fluxes have the following functional form:

$$\begin{aligned} u_* &= \frac{\kappa(U - U_0)}{\ln(z/z_0) - \Psi_m(z/L)}, \\ \frac{-\langle \theta w \rangle + \langle \theta_{sp} w \rangle}{u_*} &= \frac{\kappa(\Theta - \Theta_0)}{\ln(z/z_{0T}) - \Psi_h(z/L)}, \quad \text{and} \\ \frac{-\langle qw \rangle + \langle q_{sp} w \rangle}{u_*} &= \frac{\kappa(Q - Q_0)}{\ln(z/z_{0q}) - \Psi_h(z/L)}, \end{aligned} \quad (2.6)$$

where z_0 , z_{0T} , and z_{0q} are the reference heights for the zero mean wind, the sea surface temperature, and moisture, which are slightly above the wave height, θ_{sp} is the perturbation in potential temperature caused by the sensible heat release from sea spray, q_{sp} is the perturbation in specific humidity due to the evaporation from

sea spray, and the subscript 0 of a variable indicates the value of the variable assumed at the corresponding “surface” reference height (z_0 , z_{0T} , or z_{0q}). It should be pointed out that the premise of the argument behind these functional forms is that the Monin–Obukhov similarity relations hold in the possible range of surface winds above the wave height and, in particular, the existence of spray over breaking waves does not invalidate them. This premise is convenient since Monin–Obukhov similarity formulations for surface momentum and heat fluxes are commonly used in numerical weather prediction models.

It is further assumed that the wind in the hurricane surface boundary layer is strong enough to render $z \ll |L|$ [i.e., the vertical profiles of wind, temperature, and moisture are slightly departed from those associated with the neutral stability and the departure is linearly dependent on z/L ; see p. 50 in Garratt (1992)]. Then, the stability functions in the above flux formulations can be approximately partitioned into two parts: one is related to L_{MO} and the other is related to L_{sp} (i.e., $L^{-1} = L_{MO}^{-1} + L_{sp}^{-1}$, where $L_{MO} = -[u_*^3/\kappa(g(\theta_v w)/\Theta_v)]$ and $L_{sp} = -\{u_*^3/\kappa[g(\theta_{v,sp} w)/\Theta_v - g\sigma V_f S]\}$). That is, the assumption leads to the following approximations:

$$\Psi_m(z/L) \approx \Psi_m^{(1)}(z/L_{MO}) + \Psi_m^{(2)}(z/L_{sp}) \quad (2.7a)$$

and

$$\Psi_h(z/L) \approx \Psi_h^{(1)}(z/L_{MO}) + \Psi_h^{(2)}(z/L_{sp}), \quad (2.7b)$$

where superscripts (1) and (2) denote the two partitioned functions that are dependent on z/L_{MO} and z/L_{sp} , respectively. In sections 3 and 4, parameterizations of the sea-spray modification to the surface momentum and heat fluxes are developed separately based on these approximations.

In summary, the challenge of parameterizing how sea spray modifies the surface momentum and heat (and moisture) fluxes lies in the determination of the stability functions associated with L_{sp} . Nonzero stability functions indicate nonneutral stratification and result in departures of the wind speed, temperature, and moisture profiles from the so-called neutral ones. Since it is shown above that the effect of sea spray can be accounted for in the stability functions for the surface momentum and heat (and moisture) fluxes, the parameterizations of the effect can be derived separately from the determination of the departures from the neutral profiles using the principle of the enthalpy conservation and the steady budget equation of TKE. The parameterized effect is

then implemented together in NWP models consistently according to Eqs. (2.6) and (2.7) to account for the combined effect of sea spray on the surface momentum and heat (and moisture) fluxes.

3. Parameterization of the sea-spray effect on the heat fluxes

Consider a vertically uniform air column of depth D above the sea surface that has a unit horizontal area. In NWP models, D refers to the lowest model level where surface fluxes are defined and calculated. When the Monin–Obukhov similarity theory is used to calculate the momentum and heat (and moisture) fluxes between the sea surface and elevation $z = D$, Eqs. (2.6) and (2.7) in section 2 indicate that the overall thermal feedback effect of sea spray on the heat fluxes is to induce changes to the profiles of wind speed, temperature, and moisture of the air below the level $z = D$. Using δT_a and δQ_a to denote the average changes of the air temperature and moisture in the column, the goal of the parameterization of the thermal feedback effect of sea spray is to relate δT_a and δQ_a to the mean wind speed U , temperature T_a , and moisture Q_a in the column. Following Andreas and Emanuel (2001), the principle of enthalpy conservation is used to determine δT_a and δQ_a .

Let T_s denote the sea surface temperature and assume that the column consists of dry air mass m_d and water vapor mass m_v . If the wind speed at the top of the column is high enough to convert a small amount of sea-water mass δm_i into spray droplets, the conservation of enthalpy in the air–sea coupled system requires that the following equation holds:

$$\begin{aligned} [c_{pd}m_d + c_{pv}(m_v + f_e\delta m_i)]\delta T_a + L_v f_e \delta m_i \\ = c_w \delta m_i [(T_s - T_a) + (1 - f_e)(T_a - T_w)], \end{aligned} \quad (3.1)$$

where f_e is the fraction of δm_i that evaporates; c_{pd} , c_{pv} , and c_w are the heat capacity of dry air, water vapor, and seawater, respectively; T_w is the mean wet-bulb temperature in the column; and L_v is the latent heat of vaporization.

If we let ρ_d and ρ_v be the mean densities of dry air and water vapor in the column, Eq. (3.1) can be written as

$$\begin{aligned} [c_{pd}\rho_d + c_{pv}(\rho_v + f_e\delta m_i/D)]\delta T_a + L_v f_e \delta m_i/D \\ = c_w \delta m_i/D [(T_s - T_a) + (1 - f_e)(T_a - T_w)]. \end{aligned} \quad (3.2)$$

Equation (3.2) immediately leads to the expression of the air temperature perturbation due to the spray injection and evaporation as follows:

$$\delta T_a = \frac{c_w \delta m_i / D [(T_s - T_a) + (1 - f_e)(T_a - T_w)] - L_v f_e \delta m_i / D}{c_{pd} \rho_d + c_{pv} (\rho_v + f_e \delta m_i / D)} \tag{3.3}$$

Corresponding to this change in temperature is the change in water vapor mixing ratio, $\delta Q_a = f_e \delta m_i / D$ (or the change in dew temperature, δT_d , which can be obtained using δQ_a from the Clausius–Clapeyron equation). The mass variable is computed from the specified droplet mass flux, F_M , as $\delta m_i = F_M \delta t$, where δt is an adjustment time scale for the droplet evaporation layer.

After both δT_a and δQ_a are computed according to the formulations described above, the direct turbulent and sea-spray mediated sensible and latent heat fluxes (denoted with suffixes dir and sp, respectively) at $z = D$ can be written as

$$H_{s,dir} = \rho_a c_{pa} C_H U [T_s - (T_a + \delta T_a)], \tag{3.4a}$$

$$H_{L,dir} = \rho_a L_v C_E U [Q_s(T_s) - Q_s(T_d + \delta T_d)], \tag{3.4b}$$

$$H_{s,sp} = \rho_w c_w F_M [T_s - (T_w + \delta T_w)], \tag{3.4c}$$

$$H_{L,sp} = \rho_w L_v F_E [Q_s(T_a + \delta T_a) - Q_s(T_d + \delta T_d)], \tag{3.4d}$$

where ρ_a is the density of moist air; ρ_w is the density of seawater; c_{pa} and c_w are the heat capacity of air (including moisture) and seawater, respectively; $Q_s(T)$ is the gridbox mean saturation specific humidity at temperature T ; $H_{s,\chi}$ and $H_{L,\chi}$ denote the sensible and latent heat fluxes, respectively, where χ denotes the association with direct turbulence (dir) or sea spray (sp); C_H and C_E are the exchange coefficients for the direct turbulent transfer of sensible and latent heat at $z = D$, respectively; and F_M and F_E are the spray droplet mass and water-vapor fluxes, respectively, where $f_e = F_E / F_M$. Both factors F_M and F_E are specified from the droplet spectrum (see Fairall et al. 1994). Subscript dir denotes the direct turbulent fluxes without the feedback effect of sea spray that, as specified by Eqs. (3.4a) and (3.4b), are connected with the intensity of turbulence in the surface layer through the following relations among the heat exchange coefficient C_H (and C_E), the drag coefficient C_D , and the friction velocity u_* :

$$C_H = C_D^{1/2} \frac{\kappa}{\ln(z/z_{0T}) - \Psi_h(z/L_{MO})} \quad \text{and} \quad u_* = C_D^{1/2} U.$$

The friction velocity u_* , as a general measure of the intensity of turbulence in the surface layer and usually obtained according to the Monin–Obukhov similarity theory, is influenced by the suspension of sea spray (see

appendix A). The parameterization of the sea-spray influence on u_* is discussed in the next section.

4. Parameterization of the sea-spray effect on the momentum flux

The effect of sea spray on the surface momentum flux is realized through its enhancement of airflow stratification—airflow lamination under gravity—due to mass loading (see, e.g., Barnes 2008), and thus it can be dealt with following Barenblatt (1996) and Lykossov (2001). Ignoring the thermal effect of sea spray, the solution of the simultaneous steady equations of droplet mass conservation and TKE budget leads to the following expression of friction velocity at the level of D , the depth of the column referred to in section 3 (or the lowest model level) above the mean sea level (see details in appendix A):

$$u_* = \frac{\kappa U}{\ln\left(\frac{D}{z_0}\right) - \Psi_s},$$

$$-\Psi_s = \begin{cases} \omega^{-1} \ln\left\{1 + \frac{\alpha \omega^2}{1 - \omega} \left[\left(\frac{D}{z_0}\right)^\gamma - 1\right]\right\} & \text{for } \omega \neq 1 \\ \ln\left[1 + \alpha \ln\left(\frac{D}{z_0}\right)\right] & \text{for } \omega = 1 \end{cases}, \tag{4.1}$$

where $\gamma = 1 - \omega$, $\omega = V_f / \kappa u_*$, $\alpha = \beta g \kappa^2 z_0 \sigma S_0 / u_*^2$, $S_0 = S(z_0)$, V_f is the mean fall speed of droplets in the MSBL, σ is defined the same as in Eq. (2.2), and β is a constant associated with a linear approximation of the non-dimensional vertical gradient of mean wind (see appendix A). It is assumed for simplicity that z_0 is the level of wave breaking (i.e., spray generation). It should be pointed out that the Monin–Obukhov similarity theory is only valid at heights well above z_0 where the wave breaking takes place as revealed by the results from an explicit simulation of the impact of sea spray on the TKE budget in the surface boundary layer (Bianco et al. 2011).

Numerical implementation of the parameterizations of the sea-spray effect in NWP models requires a proper interface between the direct air–sea turbulent fluxes, which are computed using the Monin–Obukhov similarity theory, and the sea-spray effect parameterizations. In theory, calculating surface momentum and buoyancy fluxes in NWP models using the Monin–Obukhov similarity formulations requires solving the equations for the flux calculations iteratively due to the dependence

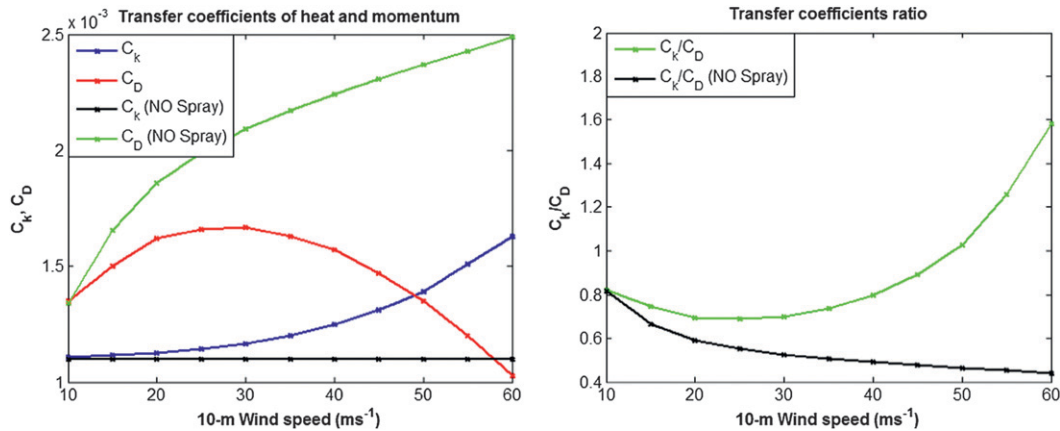


FIG. 1. (left) The 10-m neutral drag coefficient C_D and enthalpy exchange coefficient C_k as functions of 10-m wind speed following Eqs. (3.4) and (4.1). (right) The corresponding ratio of C_k/C_D .

of the fluxes on the stability functions, which in turn are dependent on the length scale L_{MO} that is defined by the surface momentum and buoyancy fluxes. Since the generation rate of sea spray is dependent on the surface momentum flux, the calculation of the sea-spray effect should be part of the iterative procedure for the surface flux calculation. One iterative procedure commonly used in NWP models is to use the surface fluxes obtained from the previous time step as the first guess for the solution at the current time. To follow this procedure, it is recommended that the above-mentioned parameterizations of the sea-spray effect be called in the code of NWP models right after the direct air–sea turbulent fluxes are calculated, so that the current spray-modified friction velocity, sensible heat, and moisture fluxes are used at the next time step in the determination of the Monin–Obukhov similarity stability functions that are required in the calculations of the direct air–sea fluxes. This will allow the interaction between the direct fluxes and the spray-mediated fluxes. Special care should also be taken in the interface when the NWP models are coupled with wave prediction models.

5. The physics of the parameterized sea-spray effect

Closing the previously discussed parameterization scheme of the effect of sea spray on air–sea exchange processes requires information on the production rate of droplets at various radii as a function of the wind speed or wave states. In this study, this information is provided through the droplet source function based on the physical model of droplet generation developed by Fairall et al. (2009). This physical model incorporates the most recent laboratory measurements and the current understanding of the turbulence energetics in wave

breaking. It predicts the size spectrum of sea-spray droplets produced by wave breaking as a function of the surface wind stress and the wave state. When implemented in an NWP model that is not coupled with a surface wave model, the wave state is diagnostically determined by the surface wind stress (Fairall et al. 2009).

Figure 1 illustrates the parameterized effect of sea spray on the 10-m drag coefficient C_D and enthalpy exchange coefficient C_k , along with their ratio (C_k/C_D), as functions of 10-m wind speed. All the exchange coefficients that include the effect of sea spray are calculated according to the formulations summarized in appendix B by prescribing 10-m wind speeds and using the bulk surface flux formulations described in Fairall et al. (1996) with modifications to include the parameterized effect of sea spray according to Eqs. (3.4) and (4.1) for 10-m wind speeds greater than 10 m s^{-1} . The wave state required for calculating the sea-spray generation is specified diagnostically by the surface wind stress. The counterparts of these coefficients and ratio without the effect of sea spray are also shown in Fig. 1 for comparison. The formulation for C_D without the sea-spray effect combines the Fairall et al. (1996) formulation for low winds and the Moon et al. (2007) formulation for high winds based on the Powell et al. (2003) observational analysis. The formulation for C_k (assuming $C_k = C_H = C_E$) without the sea-spray effect shown in Fig. 1 is based on the Fairall et al. (1996) formulation for low winds and the extrapolation of the fitting function of the CBLAST observations for high winds.

The prominent feature shown in Fig. 1 is that the increase of sea-spray mass generation with wind leads to a reduction (or an increase) in the drag coefficient (or the heat exchange coefficient) at hurricane-strength winds. The behavior of C_D with sea-spray effect as a function of the 10-m wind is consistent with recent observations

(Powell et al. 2003; Black et al. 2007; Drennan et al. 2007; French et al. 2007; Zhang et al. 2008) and the newly developed surface resistance law (Makin 2005; Andreas 2004) over rough seas associated with extreme winds, both of which show that the drag coefficient is reduced at hurricane-strength winds. The impact of sea spray on both C_D and C_k on the 10-m wind speed is insignificant until the 10-m wind speed is well above 30 m s^{-1} . The dependence of the ratio of C_k/C_D on the 10-m wind speed is consistent with C_H/C_D shown in Zhang et al. (2008) for 10-m winds below 30 m s^{-1} and in agreement with the theoretical requirement for a tropical cyclone to intensify (Emanuel 1995) for 10-m winds above 30 m s^{-1} .

The physical behavior of the scheme is consistent with the results from the explicit modeling of the TKE budget of the spray-laden surface boundary layer flow (Fairall et al. 1994; Kepert et al. 1999; Bianco et al. 2011) and the parameterized size distribution of sea-spray droplets (Fairall et al. 2009). When the 10-m wind speed is below 30 m s^{-1} , the droplets tend to be small in size and tend to evaporate substantially, and thus tend to cool the spray-filled layer. When the 10-m wind speed is well above 30 m s^{-1} , the size of droplets tend to be so big that they do not have enough time to evaporate that much before falling back into the sea. When the large droplets are still in the air, they have sufficient time to release sensible heat to the ambient air (Andreas 1990, 1995), increasing the buoyancy of the surface layer and enhancing the turbulent mixing. On the other hand, the suspension of sea-spray droplets reduces the buoyancy and makes the surface layer more stable, lowering the friction velocity and the downward turbulent mixing of momentum is reduced. The overall effect of these two processes is to increase the enthalpy exchange coefficient and reduce the drag coefficient at high winds ($>30 \text{ m s}^{-1}$). The fact that sea-spray affects the intensity of turbulence at hurricane-strength winds has an implication in the quantitative evaluation of the feedback effect of sea spray. That is, although the reduction (or increase) in the drag coefficient (or the heat exchange coefficient) at winds greater than 30 m s^{-1} depends only on the total mass and size distribution of sea-spray mass generation and is independent of which bulk scheme is used, the total momentum and enthalpy fluxes are dependent on how the direct turbulent fluxes are calculated.

It should be pointed out that the parameterizations of the sea-spray effect are different from the previous ones (e.g., Fairall et al. 1994; Andreas 2004; Makin 2005) in that the influence of sea spray on the air–sea momentum, sensible heat, and moisture fluxes is simultaneous. It is also worth noting that, although the qualitative characteristics of the above parameterizations are physically

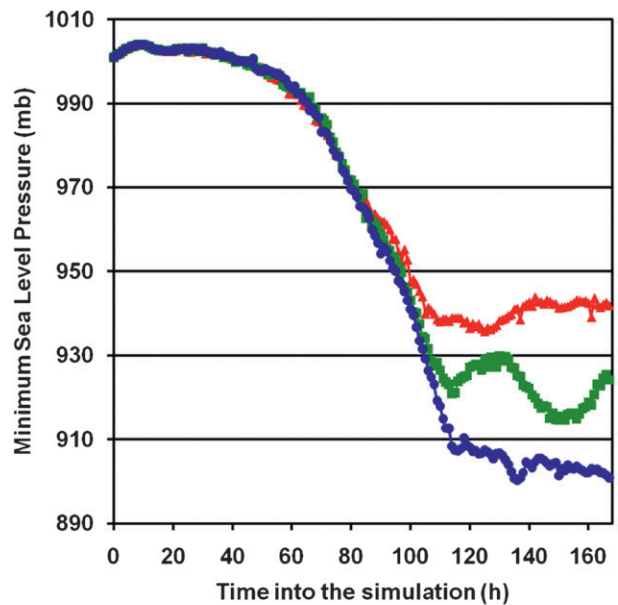
and dynamically reasonable in comparison with the observational evidence from Black et al. (2007) and Zhang et al. (2008), the quantitative aspects of the parameterizations are subject to uncertainties due to the lack of observations to validate the spray generation function and the effect of droplets on the air–sea momentum and enthalpy fluxes. Furthermore, by using the Monin–Obukhov similarity framework, the derivation of the parameterizations uses the assumptions about the steadiness and horizontal homogeneity of turbulent flow in the surface boundary layer of tropical cyclones. Admittedly, these assumptions may not be valid in the hurricane surface boundary layer. Despite the fact that the Monin–Obukhov similarity theory is widely accepted in the meteorological community for surface turbulent flux calculations in NWP models, the steadiness and horizontal homogeneity assumptions may impose a fundamental limitation on the validity of using the Monin–Obukhov similarity theory in NWP models for tropical cyclone prediction. Thus, the validity of our parameterization scheme is inevitably affected by such a limitation. There are also intrinsic uncertainties in the physical model on which the formulation of the spray generation function is based. In the parameterization of the sea-spray impact on the surface momentum flux [Eq. (4.1)], the formulation for the so-called fall speed is used to estimate the fall speed at a given elevation for a given size of droplet. It may not be appropriate to assume that all the droplets will reach the steady fall speed before they fall back to the sea. Detailed observations are required to reduce these uncertainties. It is expected that the quantitative aspects of the parameterizations will continue evolving as future observations, along with the increasing theoretical knowledge of the interaction between turbulence and sea-spray droplets, become available. Nevertheless, the conceptual framework presented here will continue to be useful for properly taking into account the effect of sea spray in the air–sea momentum and heat transfer that is formulated in accordance with the Monin–Obukhov similarity theory.

6. Sensitivity of an NWP model to the parameterizations

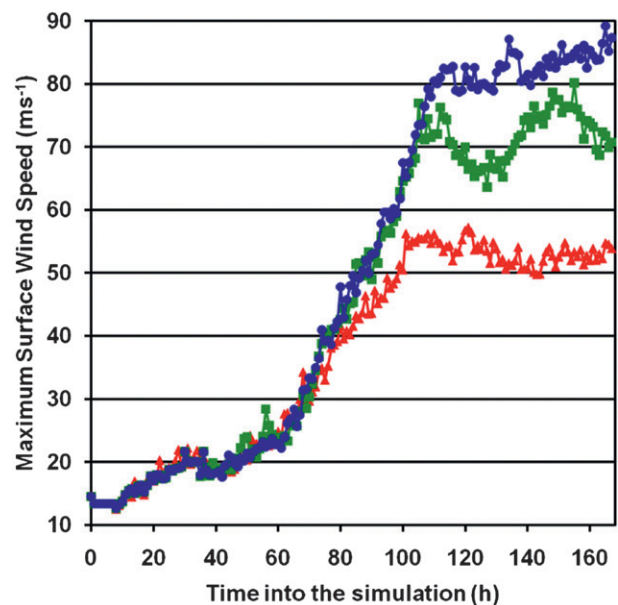
To demonstrate the impact of the aforementioned sea-spray parameterizations on an intensifying tropical cyclone, sensitivity simulations are conducted using the 3.0.1.1 version of the Weather Research and Forecasting (WRF) model initialized with an idealized vortex. The WRF model is a nonhydrostatic, fully compressible mesoscale model (Skamarock et al. 2008). A cyclone-centered moving grid of 3-km grid spacing and 241×241 grid points, which is nested in a steady outer 9-km grid, is

used for all the simulations. The outer 9-km grid has 481×481 grid points. There are a total of 43 vertical levels with the model top at 50 mb. To initialize the idealized vortex, the nonlinear balance equation in the pressure-based sigma coordinate system described in Wang (1995) is solved within the WRF-grid framework on an f plane located at 12.5°N . The mass field is derived from the wind field corresponding to an axisymmetric cyclonic vortex of maximum surface tangential wind set to 15 m s^{-1} at 280 km from the vortex center that is embedded in a quiescent flow. The far field temperature and humidity are based on Jordan's Caribbean sounding (Gray et al. 1975). In all of the experiments, the sea surface temperature was set to 302.16 K. All the experiments were run for 7 days. The physics options used in the simulations on both grids include the Yonsei University atmospheric boundary layer scheme; the WRF 6-class single-moment microphysics scheme, which has prognostic equations for water vapor, cloud water, rain, cloud ice, graupel and snow; the Dudhia simple shortwave scheme; and the Rapid Radiative Transfer Model (RRTM) longwave scheme. No convective parameterization scheme is used. It is worth mentioning that in the surface flux scheme coupled with the Yonsei University atmospheric boundary layer scheme, the roughness length z_0 for momentum flux is specified using the Chanock relationship, while the roughness length z_{0h} for the sensible and latent heat fluxes is defined through a friction-velocity Reynolds number (defined as $u_* z_{0h} / \nu$, where u_* is the friction velocity and ν is the molecular viscosity of air). Four stability regimes are considered in the formulations of the stability functions. Details of all the physics schemes including corresponding references are available in Skamarock et al. (2008).

The impact of the parameterized sea-spray effect on the simulated minimum sea level pressure and maximum surface wind speed (defined at the lowest model level, which is about 30 m above the sea surface) is demonstrated by comparing three sensitivity runs (Fig. 2). The first run, in which the sea-spray parameterization is not included, is named the control. In the second run (named the no-impact-on-heat run), only the feedback impact of sea spray on the surface momentum flux (i.e., the friction velocity u_*) is taken into account. The full impact of sea spray on both the surface momentum and heat fluxes is taken into account in the third run (named the full-impact run). There are significant differences in the intensity of the simulated hurricane. In all 3 runs, the simulated cyclone intensification rate starts to slow down and level off by 100 h after the initial time. During this period of reduced intensification rate (100–160 h), the minimum sea level pressure is about 40 mb lower, and the maximum surface wind speed is about 30 m s^{-1} faster in



(a)



(b)

FIG. 2. (a) Minimum sea level pressure (mb) and (b) maximum surface wind speed (m s^{-1}). The control run (without the sea-spray parameterization) is in red, the no-impact-on-heat run (with the feedback of sea spray to the momentum flux only) is in green, and the full-impact run (with the feedback of sea spray to both momentum and heat fluxes) is in blue.

the full-impact run than in the control run. In the no-impact-on-heat run, the maximum surface wind speed is about 20 m s^{-1} faster than the control run, while the minimum sea level pressure is 20 mb lower.

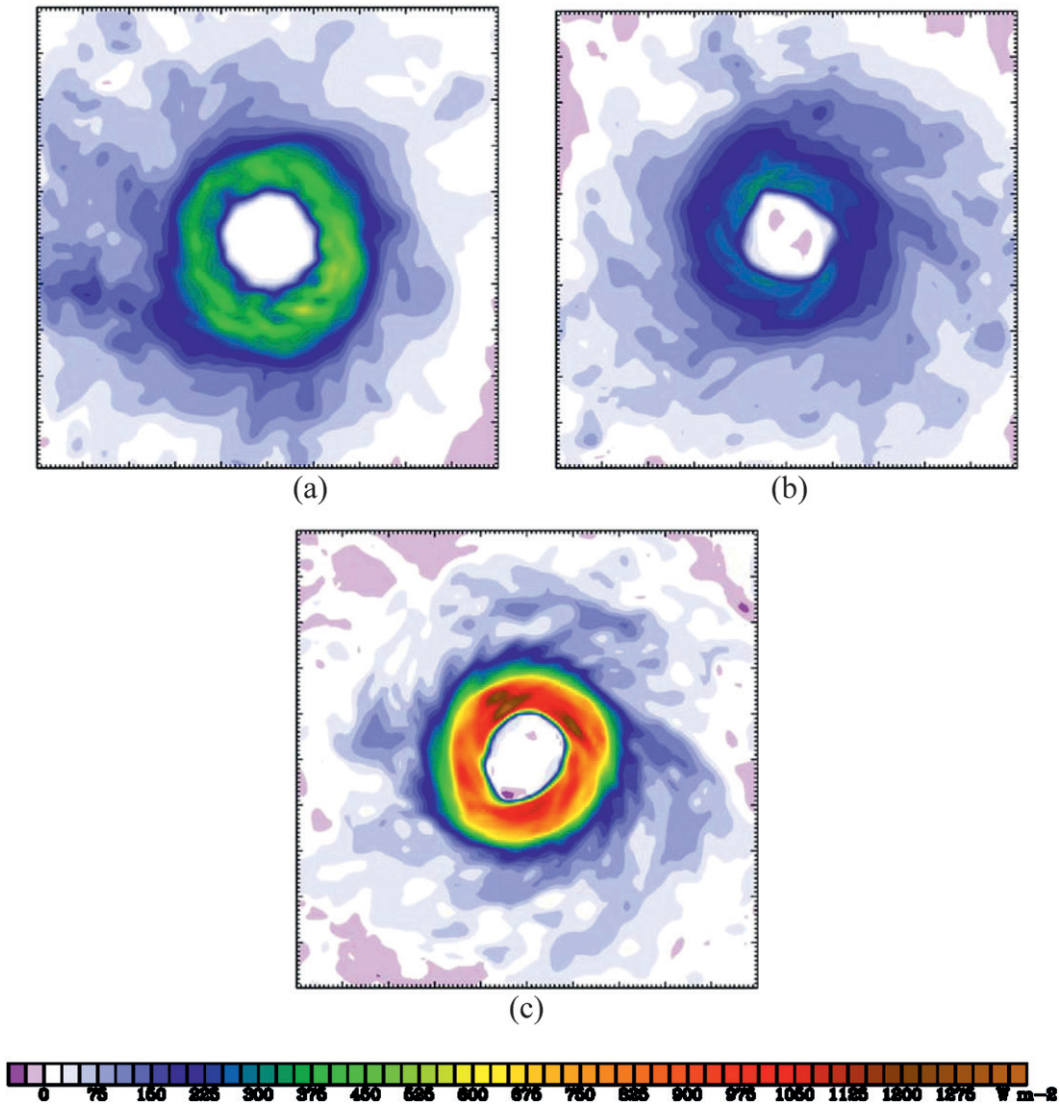


FIG. 3. The surface sensible heat flux (W m^{-2}) valid at 120 h into the simulation from (a) the control run, (b) the no-impact-on-heat run, and (c) the full-impact run. The size of the plotting area is $300 \text{ km} \times 300 \text{ km}$ with short tick marks separated by 3 km and long tick marks by 30 km.

The differences made by the inclusion of the sea-spray effect in the surface sensible heat, moisture, and momentum fluxes are shown in Figs. 3–5 valid at 120 h after the initial time. The momentum flux is shown in terms of the friction velocity. At this hour, the surface fluxes are significantly different due to the feedback of sea spray to the cyclone intensification. In the no-impact-on-heat run, the surface heat fluxes are reduced corresponding to the reduction in the turbulence intensity associated with the reduced surface momentum flux (cf. Figs. 3b–5b and 3a–5a). In the full-impact run, the effect of sea spray increases the maximum sensible and latent heat fluxes significantly near the center of the cyclone (see Figs. 3c

and 4c). The maximum sensible heat flux in the full-impact run is about 2 times greater than the control and the maximum latent heat flux is about 10% greater than the control. The differences in the sensible and latent heat fluxes also indicate that there is an increase of effective areal air–sea interface caused by spray droplets. The surface momentum flux in terms of the friction velocity from the full-impact run is reduced by about 35% compared to the control run. The increase in the heat fluxes and decrease in the momentum fluxes are consistent with the trend in the dependence of the drag and heat exchange coefficients on wind speed that is shown in Fig. 1. These results support the notion that sea spray

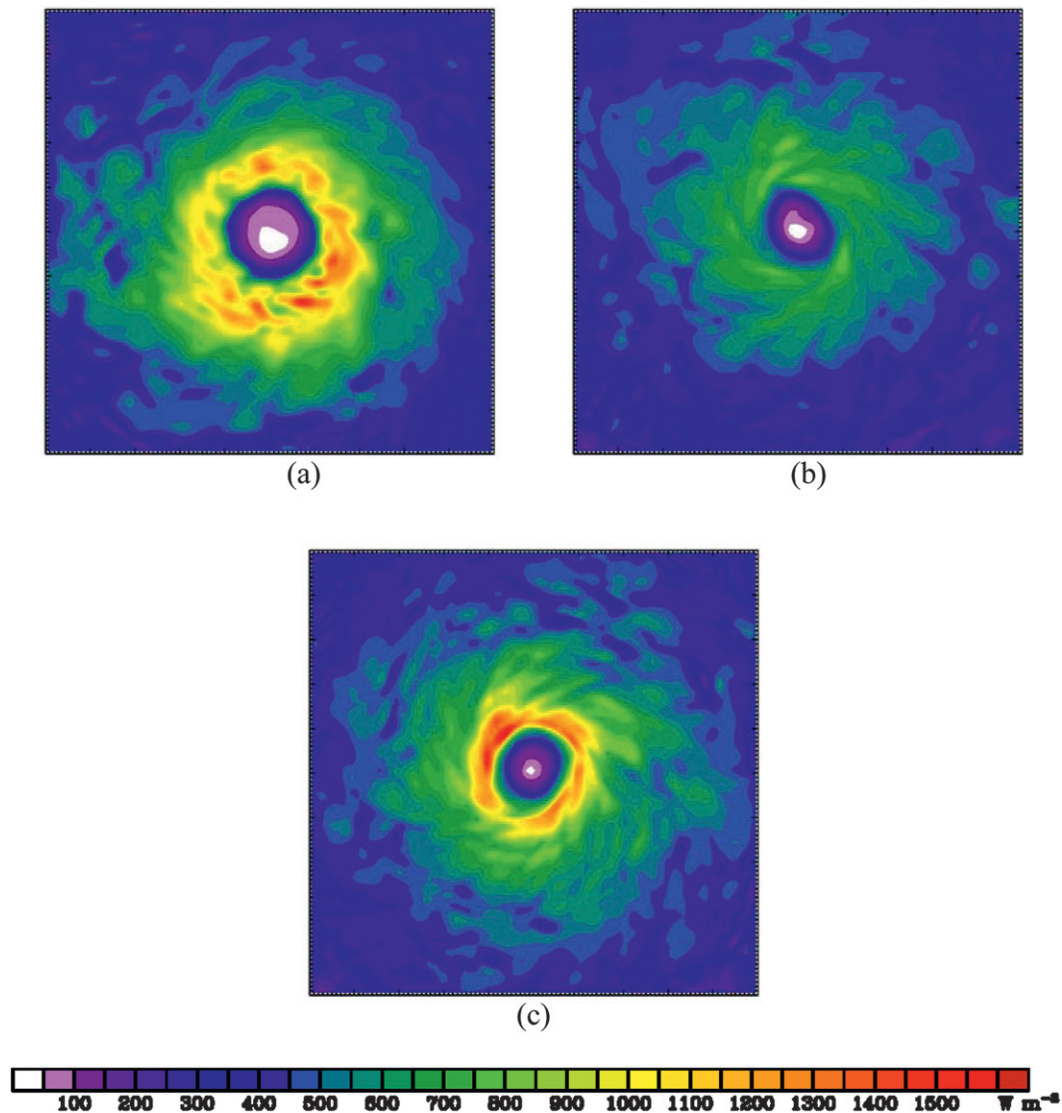


FIG. 4. As in Fig. 3, but for latent heat flux.

plays an important role in turbulent mixing near the air-sea interface. It should be noted that the differences in the surface fluxes are also the consequence of the difference in the near-surface wind distribution that is caused by the suspension and evaporation of spray droplets.

Figure 6 compares the hourly time series of the sensible heat flux, latent heat flux, and frictional velocity at the surface for the 3 runs that are averaged over a $150 \text{ km} \times 150 \text{ km}$ box centered on the cyclone center. It is seen that the full-impact run has the greatest mean sensible and latent fluxes after about 100 h, while the no-impact-on-heat run has the least mean latent heat flux, but similar mean sensible heat flux as compared to the control run. Both runs with sea spray included have lower frictional velocities than the control, with the

no-impact-on-heat run having the lowest frictional velocity. These time series confirm the overall effect of sea spray on the surface fluxes when the surface wind speed exceeds 40 m s^{-1} and the sea-spray production is significant enough to reduce the momentum flux but enhance the sensible and latent heat fluxes. The time series of the friction velocity clearly indicates that the mass loading of sea spray in the MSBL reduces the intensity of turbulent mixing, leading to the friction velocity in both runs with sea-spray effect being smaller than the control run.

Figure 7 illustrates the impact of sea spray on the azimuthally averaged structure of the ABL near the simulated cyclone center averaged from 100 to 160 h into the simulation for the 3 runs. This is the time period in all

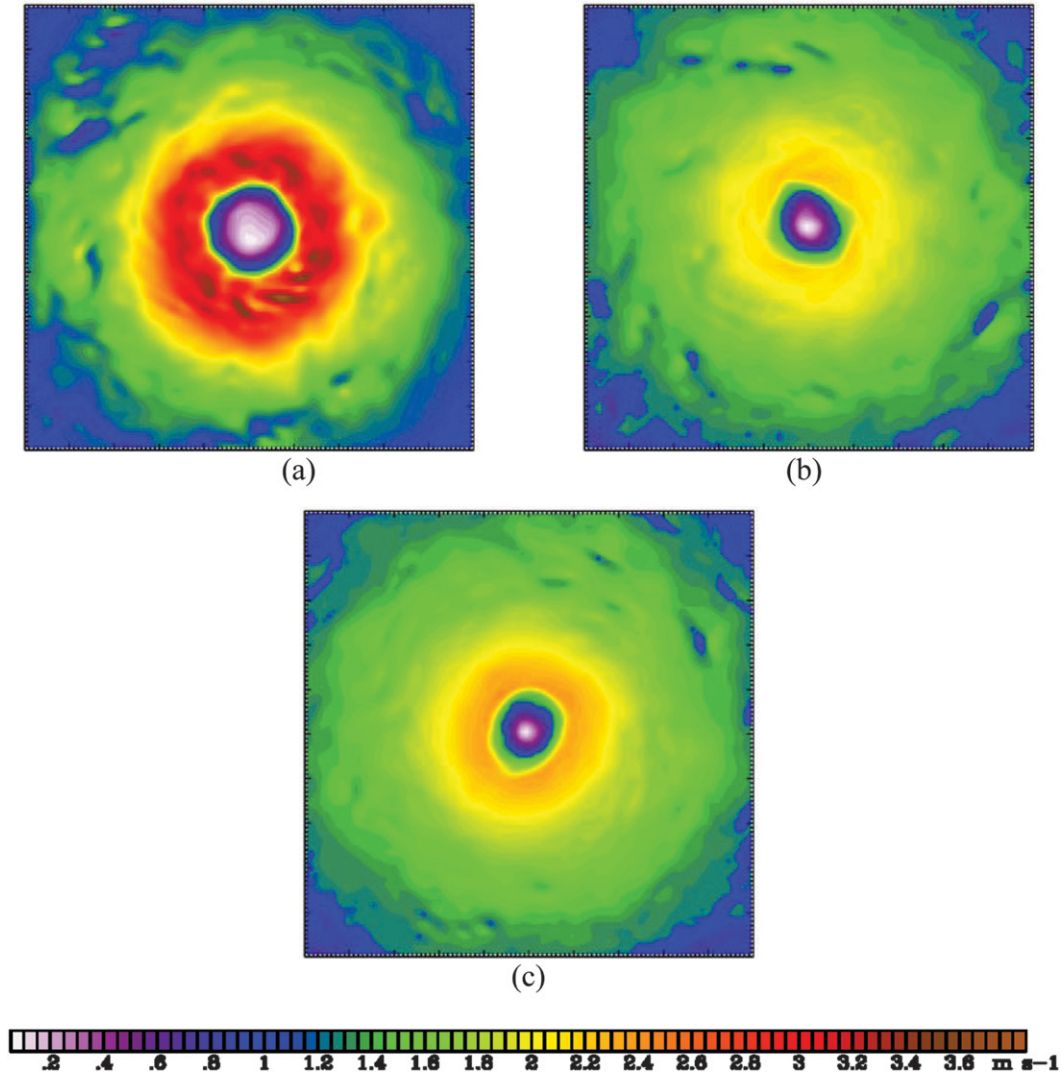


FIG. 5. As in Fig. 3, but for the momentum flux in terms of the frictional velocity (m s^{-1}).

3 simulations where the cyclone intensity begins to level off. Here, following Smith et al. (2009), the ABL near the cyclone center is defined as the layer of the near-surface inflow. In all 3 runs, the maximum tangential wind speed is within the upper part of the ABL. However, there are differences in the depth the ABL near the maximum tangential wind speed. The ABL depth within the eyewall is greater in the control and the full-impact runs than in the no-impact-on-heat run (about 1.2 km in the control and the full impact runs vs 1 km in the no-impact-on-heat run). This suggests that the ABL depth in the eyewall tends to be decreased by the increase in the flow stability due to the sea-spray mass loading, but is increased by the spray-enhanced total enthalpy flux from sea to air. That is, the effect of spray mass loading and enthalpy flux enhancement on the ABL depth in the

eyewall is opposite. It is also obvious that the sea spray decreases the radius of maximum near-surface tangential wind speed, but increases the intensity of the radial inflow. This leads to a physical interpretation for the positive impact of sea spray on the simulated cyclone intensification: the mass-loading of sea spray decreases the surface drag, which reduces the dissipation of the cyclone rotation, while the sensible and latent heat fluxes from the sea to the air are enhanced by sea spray and increase the buoyancy for deep convection in the cyclone, which intensifies the cyclone.

Figure 8 depicts the azimuthally and temporarily averaged radius–height cross sections of equivalent potential temperature θ_e within the lowest 3 km around the eyewall region for the 3 runs. These cross sections exhibit characteristics of a mature hurricane that are consistent

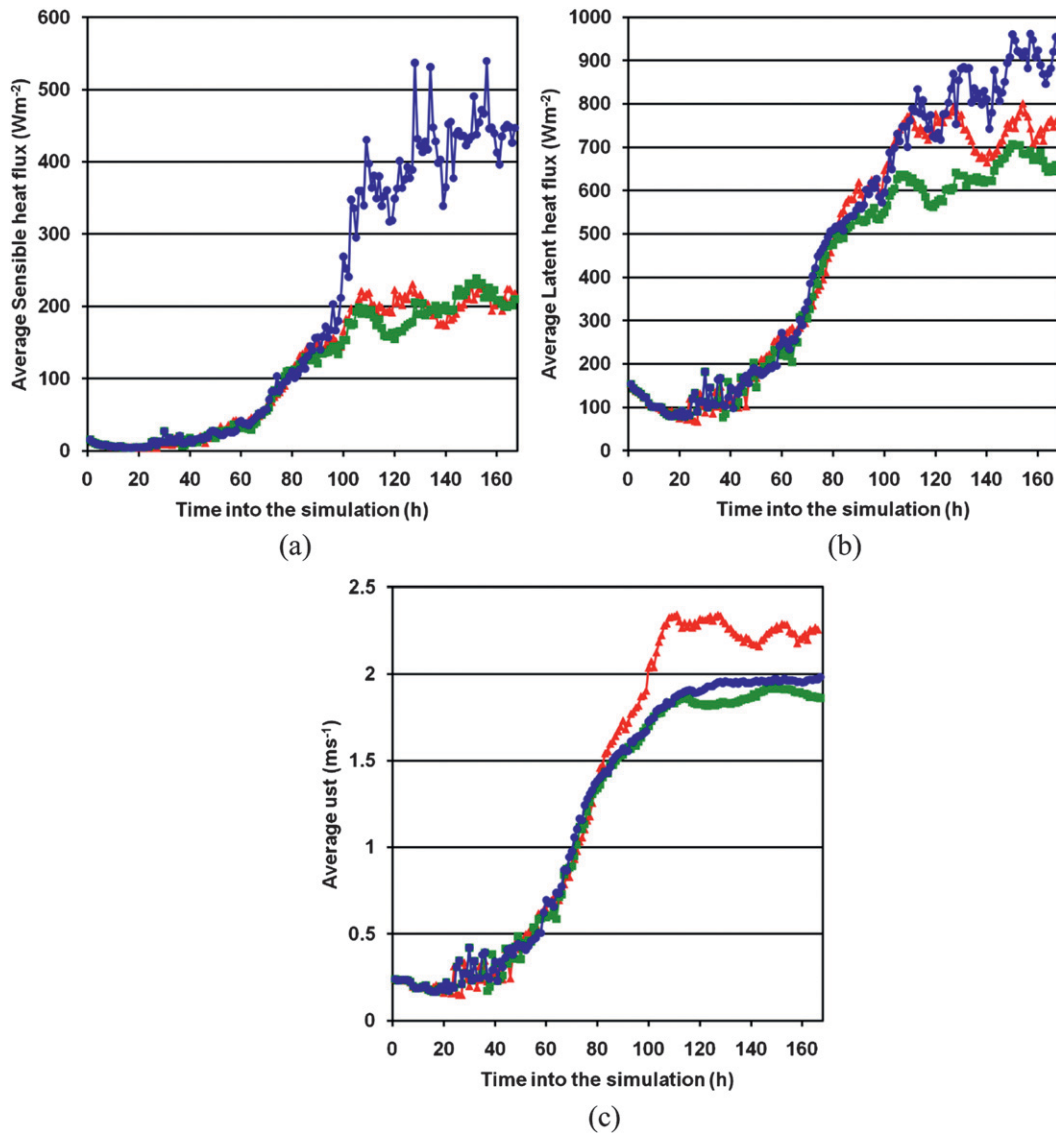


FIG. 6. Time series of (a) sensible heat flux (W m^{-2}), (b) latent heat flux (W m^{-2}), and (c) friction velocity (m s^{-1}) at surface averaged over a $150 \text{ km} \times 150 \text{ km}$ box that is centered on the cyclone. The red line is the control run, the blue line is the full-impact run, and the green line is the no-impact-on-heat run.

with the low-level thermal structure of a mature hurricane eyewall shown by Rotunno and Emanuel (1987), Persing and Montgomery (2003), and Houze (2010, section 6). The change in the slope of θ_e surfaces between the inflow and the outflow is the result of convection in the eyewall transporting higher θ_e air from the surface into the eyewall (characterized by the maximum of the outflow above the inflow in the MSBL). The radial gradient of θ_e near the surface corresponds to the radial pressure gradient associated with the cyclone intensity. When the radial gradient of θ_e increases, the surface pressure at the cyclone center decreases and the winds at the surface strengthen. Thus, the differences in the radial gradient

of θ_e near the surface clearly show that not only the intensity of the cyclone, but also its near-surface thermal structure, is strongly influenced by the sea-spray modification to the air-sea momentum and enthalpy fluxes.

7. Summary and conclusions

A parameterization scheme suitable for numerical weather prediction models has been developed to account for the effect of sea spray on the surface momentum and heat fluxes. This scheme is based on the conventional Monin–Obukhov similarity theory, which is a common framework for computing air–sea fluxes in numerical

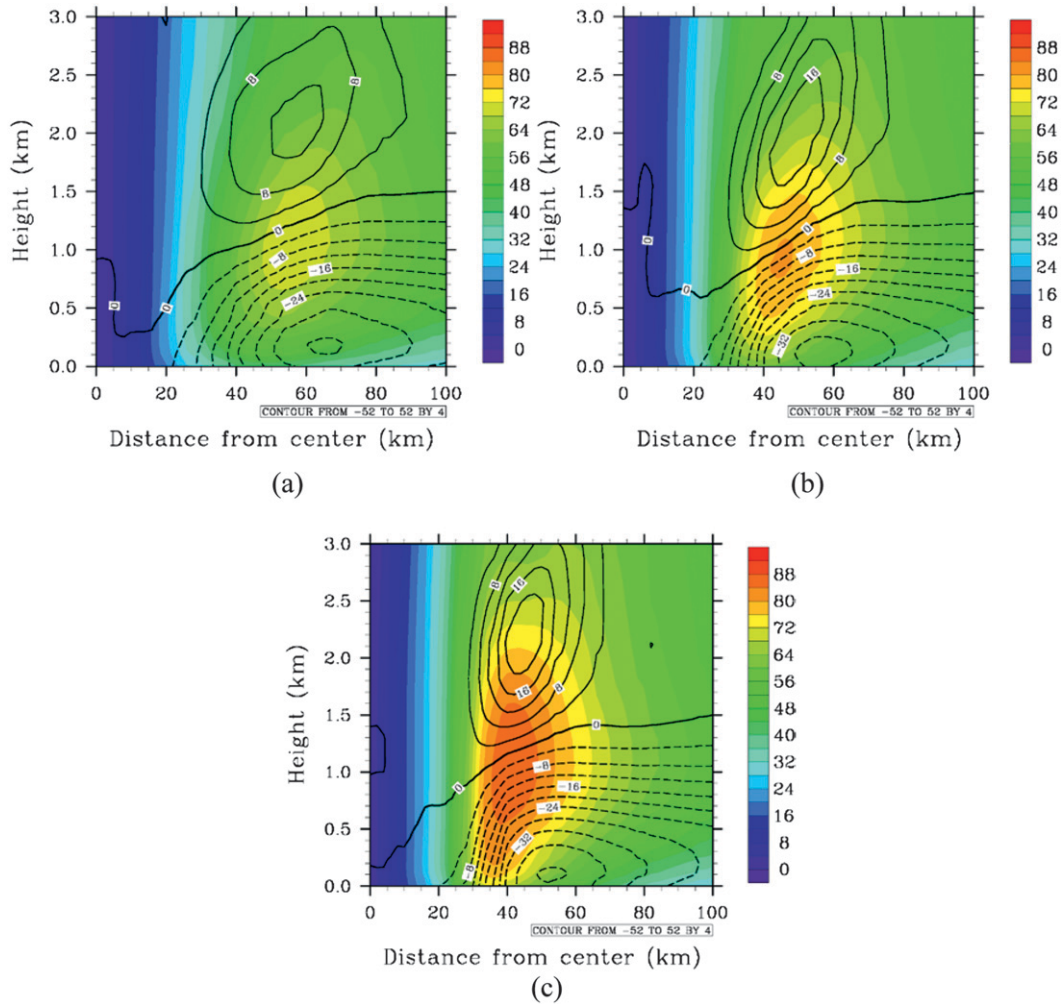


FIG. 7. Radius–height cross sections of azimuthally averaged tangential and radial wind components in the lowest 3 km averaged over 100–160 h after the initial time for the (a) control run, (b) no-impact-on-heat run, and (c) full-impact run. The color shaded contours are the tangential wind component (4 m s^{-1} interval), while the contour lines are the radial wind component (4 m s^{-1} interval and the negative indicates the direction toward the cyclone center).

weather prediction models. According to the budget equation of TKE in the spray-filled surface layer, the effect of sea spray is considered in the scheme as a modification to the stratification of the profiles of wind, temperature, and moisture in the MSBL. The scheme assumes that the Monin–Obukhov similarity relations hold in the MSBL above the elevation where wave breaking takes places and the resulting sea-spray droplets are ejected into the air.

The scheme predicts that the overall impact of sea-spray droplets on the mean winds depends on the wind speed at the level of sea-spray generation. As the wind speed increases, the average droplet size and the total mass of droplets increases, leading to an increase in the overall wind speed in the surface layer above the level of sea-spray generation. Thermodynamically, the size of

droplets at hurricane-intensity winds is so large that they do not have enough time to evaporate that much before falling back into the sea. When the large droplets are still in the air, they have sufficient time to release sensible heat to the ambient air and increase the buoyancy of the surface layer and enhance the turbulent mixing. Mechanically, the suspension of sea-spray droplets reduces the buoyancy and makes the surface layer more stable. As a consequence, the friction velocity is lowered and the downward turbulent mixing of momentum is reduced. As the cyclone continues intensifying, the reduced friction velocity, however, leads to an increased shear between the surface and the flow above the surface layer, which in turn increases the shear-induced vertical mixing in the surface layer. Also, enhanced air–sea enthalpy flux provides necessary energy

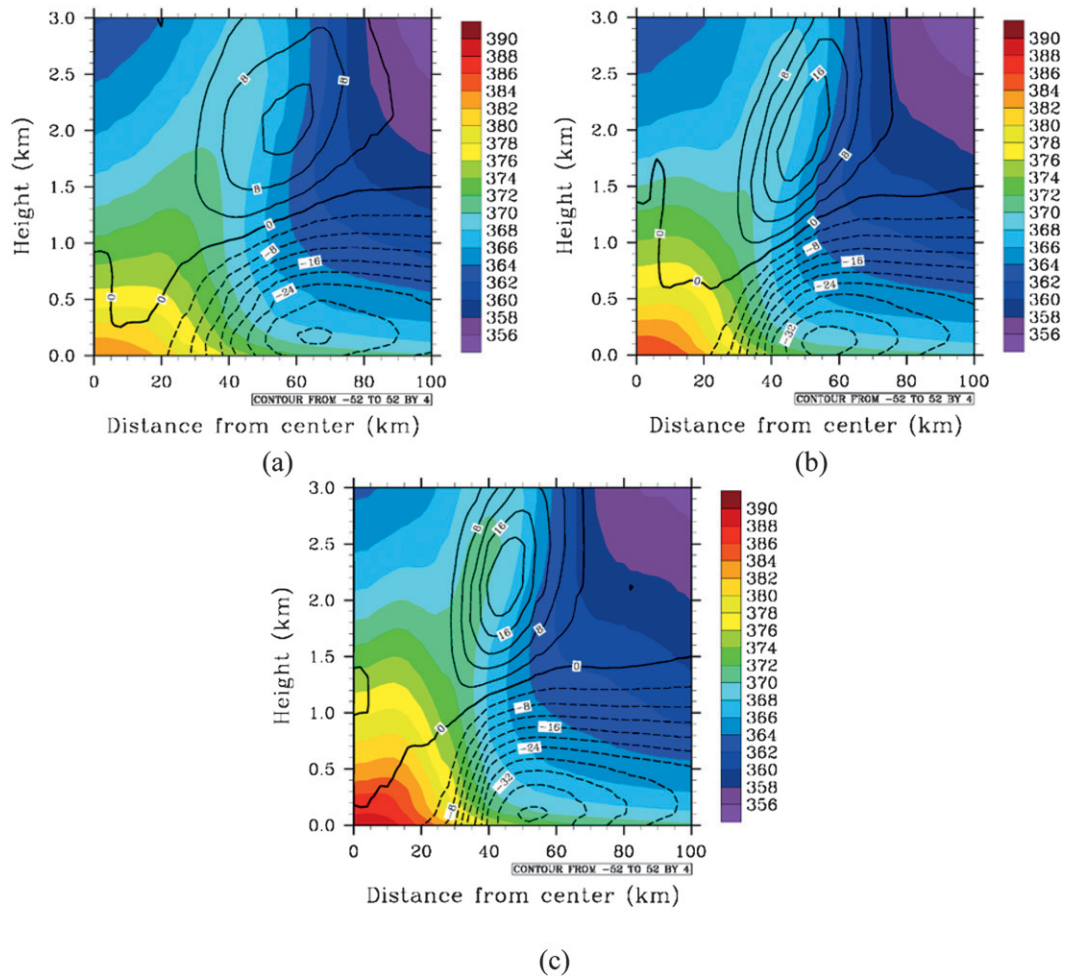


FIG. 8. As in Fig. 7, but for equivalent potential temperature and radial wind components.

to further intensify the cyclone, which in turn induces more vertical mixing.

The testing of the scheme in the simulation of an intensifying idealized tropical cyclone using the WRF model shows that the inclusion of the scheme produces significant differences in the surface sensible heat, moisture, and momentum fluxes at winds greater than 30 m s^{-1} . Overall, the scheme increases the cyclone intensity in terms of maximum surface wind and minimum sea level surface pressure. A physical interpretation for the positive impact of sea spray on the simulated cyclone intensification is that the mass-loading of sea spray decreases the surface drag, which reduces the dissipation of the cyclone rotation, while the sensible and latent heat fluxes from the sea to the air are enhanced by sea spray to increase the buoyancy for deep convection in the cyclone, thus intensifying the cyclone.

We wish to caution that the quantitative aspects of the sea-spray parameterization scheme have considerable

room for improvement, particularly when observational technology advances enough to provide reliable and accurate measurements of sea-spray generation and its interaction with the near-surface turbulence above surface waves. Thus, although the WRF model's response to the sea-spray parameterization scheme in the idealized simulation is physically consistent in terms of the scheme's prediction of the influence of sea spray on the air-sea momentum and enthalpy fluxes, the quantitative aspects of the sea-spray impact on the development of tropical cyclones are inevitably inconclusive. It is still unknown how in reality the physics of sea spray affect the ABL structure and turbulence characteristics associated with the inflow boundary layer and the outer rainbands of hurricanes that have been documented observationally (Powell 1990a,b; Barnes and Powell 1995; Zhang et al. 2009). A key shortcoming of the sensitivity experiments presented in this paper is the lack of fully coupled air-sea interaction physics in the sensitivity simulations. Further

WRF simulations with the combined sea-spray physics and the oceanic vertical mixing physics are currently being investigated, and the results revealing the sea-spray effect on the air–sea interfacial characteristics such as those described by observations in the hurricane environment (Barnes and Powell 1995; Cione et al. 2000) will be reported on in a future paper.

Hurricane development is dynamically controlled by several processes, one of which is air–sea interaction. The parameterized sea-spray effect is just one important aspect of the air–sea interaction processes. Wave breaking, which is a critical component of surface wave dynamics and a root cause for sea-spray generation, is parameterized in the current scheme to be dependent on surface wind stress only. The dynamic link between sea-spray generation and wave state as output from a coupled atmosphere–wave–ocean modeling system is not addressed in this study. While it is conceptually straightforward, how to numerically couple the current parameterization scheme of sea-spray effect with the wave model in a fully coupled modeling system, in which wave breaking, sea-spray generation, and air–sea energy transfer are interacting dynamically, remains a challenging research subject.

Acknowledgments. This work is supported by the Hurricane Forecasting Improvement Project (HFIP) of NOAA. We also thank the reviewers of this article for their insightful comments and suggestions.

APPENDIX A

Derivation of Eq. (4.1)

The steady equation of sea-spray droplet mass conservation is in the following form:

$$K_S \frac{\partial S}{\partial z} + V_f S = 0, \tag{A.1}$$

where S is the volume concentration of droplets, V_f is the fall speed of droplets, and K_S is the eddy diffusivity for droplets. Following the discussions in section 2, the steady equation of the TKE budget can be expressed as

$$\frac{\partial U}{\partial z} = \frac{u_*^3}{\kappa z} \phi_M \left(\frac{z}{L} \right), \tag{A.2}$$

where L is defined by Eq. (2.4). In the case of thermally neutral stratification (i.e., $\langle \theta, w \rangle = 0$), L becomes

$$L = \frac{u_*^3}{\kappa g \sigma \langle sw \rangle}, \tag{A.3}$$

where s is the perturbation of the volume concentration of droplets. Following Eq. (A.1) (i.e., $\langle sw \rangle = -K_S(\partial S/\partial z) = V_f S$), one can rewrite the definition of L as

$$L = \frac{u_*^3}{\kappa g \sigma V_f S}. \tag{A.4}$$

Under the stable stratification condition, since it is common to use the following approximation:

$$\phi_M \left(\frac{z}{L} \right) \approx 1 + \beta \frac{z}{L},$$

where β is a constant, Eq. (A.2) can be written as

$$\frac{\partial U}{\partial z} = \frac{u_*}{\kappa z} \left(1 + \frac{\beta \kappa g \sigma V_f S z}{u_*^3} \right). \tag{A.5}$$

Under the assumption $K_S = K_m$, where K_m is the eddy diffusivity for U , Eq. (A.1) becomes

$$\frac{\partial S}{\partial z} + \frac{w_f S}{\kappa u_* z} \left(1 + \frac{\beta \kappa g \sigma V_f S z}{u_*^3} \right) = 0. \tag{A.6}$$

The solution to Eq. (A.6) for boundary condition $S(z_0) = S_0$ is

$$S = \frac{(1 - \omega) S_0 (z/z_0)^{-\omega}}{(1 - \omega) + \omega^2 \alpha [(z/z_0)^{1-\omega} - 1]} \quad \text{for } \omega \neq 1 \tag{A.7a}$$

and

$$S = \frac{S_0 (z/z_0)^{-1}}{1 + \alpha \ln(z/z_0)} \quad \text{for } \omega \rightarrow 1, \tag{A.7b}$$

where $\omega = V_f/\kappa u_*$ and $\alpha = \beta g \kappa^2 z_0 \sigma S_0 / u_*^2$. Substitution of Eq. (A.7) into Eq. (A.5) and integrating it upward from z_0 leads to Eq. (4.1).

APPENDIX B

Surface Drag and Enthalpy Exchange Coefficients with Sea-Spray Effect

Traditionally, the momentum flux at a given height above the sea surface z is expressed in terms of the friction velocity u_* that is cast according to the Monin–Obukhov similarity theory as the following:

$$u_* = \frac{\kappa U}{\ln(z/z_0) - \Psi_m(z/L_{MO})}, \tag{B.1}$$

where U is the mean wind at z and $\Psi_m(z/L_{MO})$ is the Monin–Obukhov stability function for the momentum flux and z_0 is the reference height for the zero mean wind. Following the sea-spray effect parameterization scheme described in sections 2 and 4, the effect of droplets on the momentum flux in terms of the friction velocity u_* can be added in Eq. (B.1) through the droplet stability function ($-\Psi_s$) specified by Eq. (4.1):

$$u_* = \frac{\kappa U}{\ln(z/z_0) - \Psi_m(z/L_{MO}) - \Psi_s}. \quad (\text{B.2})$$

Thus, the surface drag coefficient defined at z with the effect of sea spray included is

$$C_D = \left[\frac{\kappa}{\ln(z/z_0) - \Psi_m(z/L_{MO}) - \Psi_s} \right]^2.$$

The direct turbulent sensible and latent heat transfer coefficients defined at z with the effect of sea spray on C_D included are

$$C_H = \frac{\kappa^2}{[\ln(z/z_0) - \Psi_m(z/L_{MO}) - \Psi_s][\ln(z/z_{0T}) - \Psi_T(z/L_{MO})]} \quad (\text{B.3})$$

and

$$C_E = \frac{\kappa^2}{[\ln(z/z_0) - \Psi_m(z/L_{MO}) - \Psi_s][\ln(z/z_{0q}) - \Psi_q(z/L_{MO})]} \quad (\text{B.4})$$

where $\Psi_T(z/L_{MO})$ and $\Psi_q(z/L_{MO})$ are the Monin–Obukhov stability functions for the sensible and moisture fluxes, and z_{0T} and z_{0q} are the reference heights for the sea surface temperature T_s and moisture q_s . The “effective” transfer coefficient associated with the total enthalpy flux including the sea-spray contribution can be computed as the following in terms of quantities defined in section 3:

$$C_k = \frac{H_{s,dir} + H_{s,sp} + H_{L,dir} + H_{L,sp}}{\rho_a U [c_p(T_s - T_a) + L_v(q_s - q_a)]} \quad (\text{B.5})$$

REFERENCES

- Adams, C. E., and G. L. Weatherly, 1981: Some effect of suspended sediment stratification on an oceanic bottom boundary layer. *J. Geophys. Res.*, **86**, 4161–4172.
- Andreas, E. L., 1990: Time constants for the evolution of sea spray droplets. *Tellus*, **42B**, 481–497.
- , 1995: The temperature of evaporating sea spray droplets. *J. Atmos. Sci.*, **52**, 852–862.
- , 2004: Spray stress revisited. *J. Phys. Oceanogr.*, **34**, 1429–1440.
- , and K. A. Emanuel, 2001: Effect of sea spray on tropical cyclones intensity. *J. Atmos. Sci.*, **58**, 3741–3751.
- Bao, J. W., J. M. Wilczak, J. K. Choi, and L. H. Kantha, 2000: Numerical simulations of air–sea interaction under high wind conditions using a coupled model: A study of hurricane development. *Mon. Wea. Rev.*, **128**, 2190–2210.
- Barenblatt, G. I., 1996: *Scaling, Self-Similarity, and Intermediate Asymptotics: Dimensional Analysis and Intermediate Asymptotics*. Cambridge University Press, 412 pp.
- Barnes, G. M., 2008: Atypical thermodynamic profiles in hurricanes. *Mon. Wea. Rev.*, **136**, 631–643.
- , and M. D. Powell, 1995: Evolution of the inflow boundary layer of Hurricane Gilbert (1988). *Mon. Wea. Rev.*, **123**, 2348–2368.
- Bianco, L., J.-W. Bao, C. W. Fairall, and S. A. Michelson, 2011: Impact of sea spray on the surface boundary. *Bound.-Layer Meteor.*, **140**, 361–381.
- Black, P. G., and Coauthors, 2007: Air–sea exchange in hurricanes: Synthesis of observations from the Coupled Boundary Layer Air–Sea Transfer Experiment. *Bull. Amer. Meteor. Soc.*, **88**, 357–374.
- Cione, J. J., P. G. Blasck, and S. H. Houston, 2000: Surface observations in the hurricane environment. *Mon. Wea. Rev.*, **128**, 1550–1561.
- Drennan, W. M., J. A. Zhang, J. R. French, C. McCormick, and P. G. Black, 2007: Turbulent fluxes in the hurricane boundary layer. Part II: Latent heat flux. *J. Atmos. Sci.*, **64**, 1103–1115.
- Emanuel, K. A., 1995: Sensitivity of tropical cyclones to surface exchange coefficients and a revised steady-state model incorporating eye dynamics. *J. Atmos. Sci.*, **52**, 3969–3976.
- Fairall, C. W., J. D. Kepert, and G. J. Holland, 1994: The effect of sea spray on surface energy transports over the ocean. *Global Atmos. Ocean Syst.*, **2**, 121–142.
- , E. F. Bradley, D. P. Rogers, J. B. Edson, and G. S. Young, 1996: Bulk parameterization of air–sea fluxes for TOGA COARE. *J. Geophys. Res.*, **101**, 3747–3764.
- , M. L. Banner, W. L. Peirson, W. Asher, and R. P. Morison, 2009: Investigation of the physical scaling of sea spray spume droplet production. *J. Geophys. Res.*, **114**, C10001, doi:10.1029/2008JC004918.
- French, J. R., W. M. Drennan, J. A. Zhang, and P. G. Black, 2007: Turbulent fluxes in the hurricane boundary layer. Part I: Momentum flux. *J. Atmos. Sci.*, **64**, 1089–1102.
- Garratt, J. R., 1992: *The Atmospheric Boundary Layer*. Cambridge University Press, 316 pp.
- Gray, W. M., E. Ruprecht, and R. Phelps, 1975: Relative humidity in tropical weather systems. *Mon. Wea. Rev.*, **103**, 685–690.
- Houze, R. A., Jr., 2010: Clouds in tropical cyclones. *Mon. Wea. Rev.*, **138**, 293–344.

- Jarosz, E., D. A. Mitchell, D. W. Wang, and W. J. Teague, 2007: Bottom-up determination of air-sea momentum exchange under a major tropical cyclone. *Science*, **315**, 1707–1709.
- Kepert, J. D., C. W. Fairall, and J.-W. Bao, 1999: Modeling the interaction between the atmospheric boundary layer and evaporating sea spray droplets. *Air–Sea Exchange: Physics, Chemistry and Dynamics*, G. L. Geernaert, Ed., Kluwer, 363–407.
- Lykossov, V., 2001: Atmospheric and oceanic boundary layer physics. *Wind Stress over the Ocean*, I. S. F. Jones and Y. Toba, Eds., Cambridge University Press, 58–81.
- Makin, V. K., 2005: A note on the drag of the sea surface at hurricane winds. *Bound.-Layer Meteor.*, **115**, 169–176.
- Moon, I., I. Ginis, T. Hara, and B. Thomas, 2007: Physics-based parameterization of air–sea momentum flux at high wind speeds and its impact on hurricane intensity predictions. *Mon. Wea. Rev.*, **135**, 2869–2878.
- Mueller, J. A., and F. Veron, 2009: A Lagrangian stochastic model for heavy particle dispersion in the atmospheric marine boundary layer. *Bound.-Layer Meteor.*, **130**, 229–247.
- Persing, J., and M. T. Montgomery, 2003: Hurricane superintensity. *J. Atmos. Sci.*, **60**, 2349–2371.
- Powell, M. D., 1990a: Boundary layer structure and dynamics in outer hurricane rainbands. Part I: Mesoscale rainfall and kinematic structure. *Mon. Wea. Rev.*, **118**, 891–917.
- , 1990b: Boundary layer structure and dynamics in outer hurricane rainbands. Part II: Downdraft modification and mixed layer recovery. *Mon. Wea. Rev.*, **118**, 918–938.
- , P. J. Vickery, and T. A. Reinhold, 2003: Reduced drag coefficient for high wind speeds in tropical cyclones. *Nature*, **422**, 279–283.
- Rotunno, R., and K. A. Emanuel, 1987: An air–sea interaction theory for tropical cyclones. Part II: An evolutionary study using a hydrostatic axisymmetric numerical model. *J. Atmos. Sci.*, **44**, 543–561.
- Skamarock, W. C., and Coauthors, 2008: A description of the Advanced Research WRF version 3. NCAR Tech. Note-475+STR, 113 pp.
- Smith, R. K., M. T. Montgomery, and S. V. Nguyen, 2009: Tropical cyclone spin-up revisited. *Quart. J. Roy. Meteor. Soc.*, **135**, 1321–1335.
- Stull, R. B., 1997: Reply. *J. Atmos. Sci.*, **54**, 579–579.
- Wang, Y., 1995: On an inverse balance equation in sigma-coordinates for model initialization. *Mon. Wea. Rev.*, **123**, 482–488.
- , J. D. Kepert, and G. Holland, 2001: On the effect of sea spray evaporation on tropical cyclone boundary layer structure and intensity. *Mon. Wea. Rev.*, **129**, 2481–2500.
- Zhang, J. A., P. G. Black, J. R. French, and W. M. Drennan, 2008: First direct measurements of enthalpy flux in the hurricane boundary layer: The CBLAST results. *Geophys. Res. Lett.*, **35**, L14813, doi:10.1029/2008GL034374.
- , W. M. Drennan, P. G. Black, and J. R. French, 2009: Turbulence structure of the hurricane boundary layer between the outer rainbands. *J. Atmos. Sci.*, **66**, 2455–2467.